TRANSPORT PROPERTIES AND STEEL CORROSION IN DUCTILE FIBER REINFORCED CEMENT COMPOSITES

Shinichi Miyazato[1] and Youichi Hiraishi[1]
[*1]Dept. of Civil & Environmental Engineering, Kanazawa Institute of Technology, Ishikawa, 921-8501 Japan

ABSTRACT

Ductile Fiber Reinforced Cement Composites (DFRCC) which was a material mixed the short fibers with mortar, was developed to improve the structural characteristics. However, the durability was not so clear. The object of this study was to clarify the durability for chloride or carbonation induced corrosions of DFRCC with the bending cracks. Therefore, the chloride ion penetration depth, the carbonation depth, the corrosion cell formation pattern (macrocell, microcell) and the corrosion rate were examined using 8 experimental cases, which were combined 2 types of materials (normal mortar, DFRCC), 2 types of environments (chloride, carbonation) and 2 levels of water cement rations (30%, 60%). Especially, to evaluate the macrocell and microcell corrosion rates, the special divided steel bar was embedded in the specimen. As a result; 1) The corrosion cell formation pattern of DFRCC was microcell, while that of normal mortar was macrocell. 2) The corrosion rate of DFRCC was lower than that of normal mortar. 3) The penetration of chloride ions or the carbonation depth in the crack of DFRCC was shallower than that of normal mortar. From the above results, it could be confirmed that the durability for chloride or carbonation induced corrosion of DFRCC was higher than that of normal mortar.

1 INTRODUCTION

Normal mortar is weakly destroyed. Therefore, the destruction rapidly progresses. This is very dangerous for the structural performance. To overcome this property, Ductile Fiber Reinforced Cement Composites (DFRCC) has been developed (V. C. Li [1]). Herein, this DFRCC will be explained. DFRCC is the cement composite material, which is mixed the short fibers with mortar. Recently the structural characteristics of DFRCC have been studied. As a result, it can be clarified that, 1) under the bending stress, the multiple cracks with minute width appear, as shown in Picture 1, and 2) after cracking, increasing the strain, increases the stress. That is, it has been confirmed that DFRCC improves the structural characteristics. Therefore in the future, it is expected that DFRCC is used in various uses for the construction materials. However, there is hardly examination about the durability of DFRCC to use for the actual structures. From the above backgrounds, the objective of this study is to clear the chloride ion penetration depth, the carbonation depth, the corrosion cell formation pattern and the corrosion rate at the bending cracks in DFRCC, compared to normal mortar. Therefore, the penetration tests and the corrosion tests are examined.

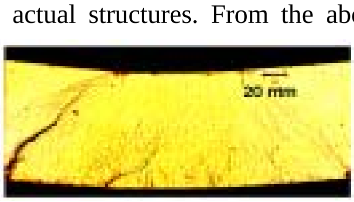

Picture 1 Multiple cracks in DFRCC

2 EXPERIMENTAL PROCEDURES

2.1 Materials and mixture proportions

Ordinary Portland cement, sand, chemical admixtures and round steel bar were used. Especially, polyethylene fiber with 12mm length and 2580MPa tensile strength was used for DFRCC. Also, the mixture proportion of DFRCC was referred to the literature (M. Kunieda [2]) and the 1.5vol% fiber was included for DFRCC.

2.2 Specimens

The specimen configurations are shown in Figures 1 and 2. The specimen for the corrosion test had the special divided steel bars in order to distinguish between the measured macrocell and microcell corrosion rates (N. Otsuki [3]). Herein, the manufacturing process of the special divided steel bar will be explained. The steel bar was composed of 13 segments which were 15mm length. The lead wires were soldered at the both ends before joining these segments with epoxy resin of high insulating capacity to form a 210-mm long bars. Also, a reinforcing bar coated with epoxy resin was set with the special divided steel bar at the tensile side. The role of this epoxy-coated reinforcing bar was to carry the bending load and produce the bending cracks without destroying the special divided steel bar. All specimens were subjected to the initial curing in the wet environment for 28days after removal from the mold. Afterwards, the bending cracks were generated by the 20kN load. As the result, in mortar specimen, the deep crack with about 0.3-0.4mm width was generated. On the other hand, the multiple shallow cracks with 0.1mm or less width were generated in DFRCC specimen. Also, the crack width was keep for the exposure period. Then, all specimens were exposed to the chloride accelerated environment for 28days or the carbonation accelerated environment for 91 days. The chloride accelerated environment was a wet-dry cycle: wet was exposure to a saltwater shower (NaCl 3.1wt %) at 90%RH for 2days, and dry was 60%RH for 5days. While, the carbonation accelerated environment was also a wet-dry cycle: wet was 90%RH for 10days, and dry was exposure to the air with high content CO_2 (CO_2 5.0 %) at 60%RH for 4days.

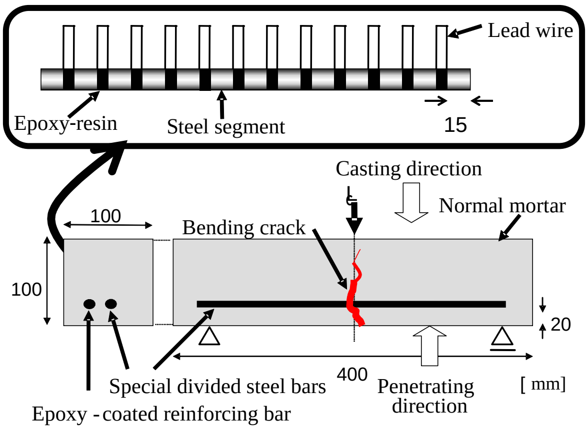

Figure 1 Specimen of mortar

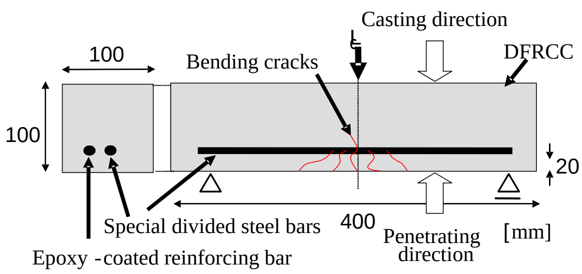

Figure 2 Specimen of DFRCC

2.3 Experimental cases

The total of experimental cases was 8, which were combined 2 types of materials (normal mortar, DFRCC), 2 types of environments (chloride, carbonation) and 2 levels of water cement rations (30%, 60%).

2.4 Measurement methods

In this study, the macrocell current referred to the current flowing in the cell composed of all steel segments. While the microcell current referred to the current flowing in the cell when only one steel segment was involved.

2.4.1 Chloride ion penetration depth

The specimen was split, and a 0.1N- $AgNO_3$aq was sprayed on the uneven surface after the steel bar was removed. Afterwards, the part which colored to the white was measured by the vernier caliper, and it was made to be “chloride ion penetration depth”. Herein, the measurement place was 3 of "uncrack division", "crack plane" and "steel bar underside", as shown in Figure 3. In case of DFRCC, the chloride ions penetration at the steel bar underside was respectively measured in multiple penetration positions, and the mean value was used.

2.4.2 Carbonation depth

The specimen was split, and a 1%- phenolphthalein alcohol solution was sprayed. Afterwards, the part which not colored to the red was measured, and it was made to be “carbonation depth”.

2.4.3 Macrocell corrosion current

The macrocell current density was determined by dividing the total electric current by the surface area. The macrocell current density (I_{macro}) for Figure 4 is shown at eqn (1).

$$I_{macro} = \frac{I_{i-1.i} + I_{i+1.i}}{S_i} \qquad (1)$$

where, I_{macro} is the macrocell current density of steel segment No.i, $I_{i-1.i}$ is the current which flows from I_{i-1} to I_i , $I_{i+1.i}$ is the current which flows from I_{i+1} to I_i, and S_i is the surface area of steel segment No.i.

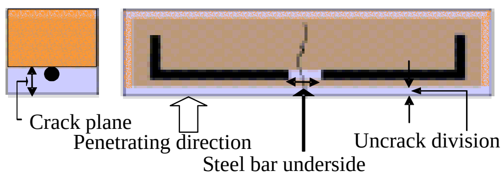

Figure 3 Measurement places of penetration depths

The anode current density is presented as positive, while the cathode current density is presented as negative.

2.4.4 Microcell corrosion current

The microcell current density was obtained from the measurement of the polarization resistance of the steel segment. The polarization resistance

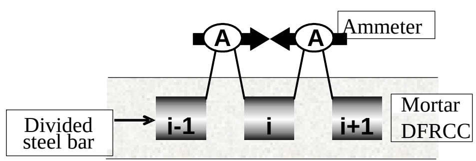

Figure 4 Measurement of macrocell current

was measured by AC impedance method with FRA (Frequency Response Analyzer) under cutting the lead wire between each steel segment, as shown in Figure 5. The microcell current density (I_{micro}) is shown at Eqn (2) (T. Tsuru [4]).

$$I_{micro} = \frac{K}{Rp_i} \qquad (2)$$

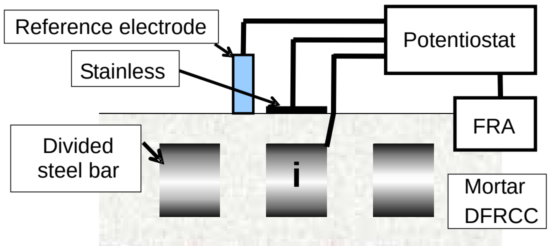

Figure 5 Measurement of polarization resistance

where, I_{micro} is the microcell current density of steel segment No.i, Rp_i is the polarization resistance of steel segment No.i, and K is 0.0209 which is a constant (T. Tsuru [4]).

2.4.5 Total corrosion rate

The corrosion rate of 1.18mm/year was changed from the corrosion current density of 100μA/cm^2. Finally, the total corrosion rate was the sum of the macrocell anode corrosion rate and the microcell corrosion rate.

3 PENETRATION TESTS

3.1 Observation examples

The observation examples are shown in Figures 6 and 7. According to these figures, chloride ions or CO_2 might penetrate into only 1 place in mortar specimen. This reason seems to be that the crack has been generated at only 1 place, as shown in Figure 1. On the other hand, chloride ions or CO_2 might penetrate into the many positions in DFRCC specimen. This reason seems to be that the cracks have been generated in the multiple positions, as shown in Figure 2.

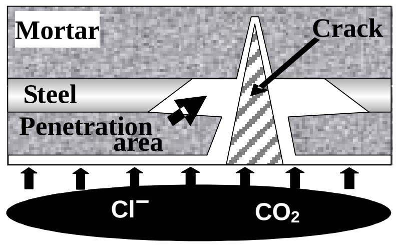

Figure 6 Penetration place in mortar

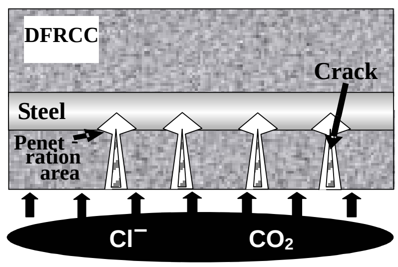

Figure 7 Penetration place in DFRCC

3.2 Results and discussions

The experimental results are shown in Table 1. According to this table, the chloride ion penetration depth and the carbonation depth at the uncrack division in DFRCC specimen may be deeper than that in mortar specimen. This reason will be discussed. It can be said that the air quantity in DFRCC is more than that in mortar, because more air-entrained agents are contained in DFRCC in order to mix

Table 1 Penetration depths

[mm]

Part	W/C (%)	Chloride ion		Carbonation	
		mortar	DFRCC	mortar	DFRCC
Uncrack division	30	5.2	4.5	0.0	0.8
	60	8.4	10.7	2.0	6.4
Crack Plane	30	83.2	0.0	97.9	21.2
	60	100.0	20.0	95.3	28.3
Steel bar underside	30	20.5	0.0	23.0	7.8
	60	31.0	22.8	34.7	8.9

without segregation. Also, it can be said that there are some interfacial transition zones between the fiber and cement matrix in DFRCC. Therefore, the chloride ion and CO_2 penetrations in DFRCC are easier than that in mortar. However, the values of the penetration depths are small in even DFRCC specimen. Also according to Table 1, the chloride ion penetration depths and the carbonation depths at the crack plane and the steel bar underside in DFRCC specimen may be shallower than those in mortar specimen. This reason will be discussed. The deeper and wider crack is generated in mortar specimen as shown in Figure 1, while the shallower and narrower cracks are generated in DFRCC specimen as shown in Figure 2. Therefore, it is difficult to penetrate chloride ions and CO_2 in DFRCC specimen, compared to mortar specimen.

4 CORROSION TESTS

4.1 Measurement examples

The examples of the corrosion rate distribution are shown in Figures 8 and 9. According to these figures, the corrosion rate is maximized at only 1 place in mortar specimen. On the other hand, the low corrosion rate appears at the multiple positions in DFRCC specimen. This reason seems to be the chloride ion penetration distribution, as described in 3.1. Next, the corrosion cell formation pattern is evaluated. That is, the highest macrocell corrosion rate is compared to the highest microcell corrosion rate. In case of mortar specimen, the macrocell corrosion rate is higher than the microcell corrosion rate. Therefore, the corrosion cell formation pattern can be judged macrocell. On the other hand, the microcell corrosion rate is higher than the macrocell corrosion rate in case of DFRCC specimen. Therefore, the corrosion cell formation pattern can be judged microcell. Finally, the corrosion rate is evaluated. The highest total corrosion rate is 0.0080mm/year in mortar specimen. While, the highest total corrosion rate is 0.0004mm/year in DFRCC specimen. Therefore, it can be judged that the corrosion rate of mortar specimen is higher than that of DFRCC specimen.

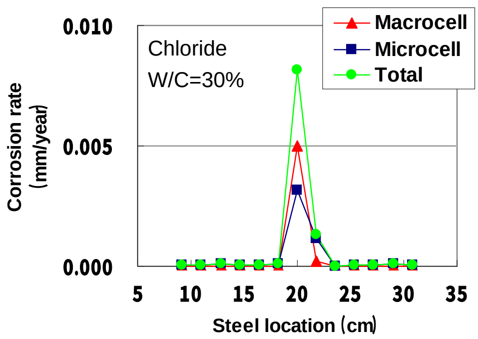

Figure 8 Corrosion rate in mortar

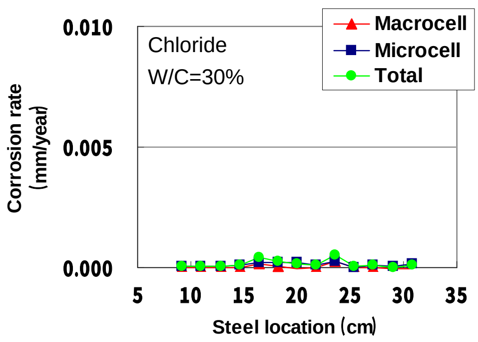

Figure 9 Corrosion rate in DFRCC

4.2 Results and discussions

The summary of the all corrosion test results is shown in Table 2. According to this table, it can be

Table 2 Summary of corrosion test results

	Mortar	DFRCC
Corrosion cell formation pattern	Macrocell	Microcell
Corrosion rate	High	Low

confirmed that the corrosion cell formation pattern of mortar specimen is macrocell, while that of DFRCC specimen is microcell. Herein, this reason is discussed. Chloride ions or CO_2 penetrate at only 1 place in mortar specimen, as described in 3.1. Therefore, macrocell is formed, because the anodic corrosion reaction is locally progressed. On the other hand, chloride ions or CO_2 penetrate at the multiple positions in DFRCC specimen, as described in 3.1. Therefore, microcell is formed, because the anodic corrosion reactions are progressed as the some positions. Also, according to Table 2, it can be confirmed that the corrosion rate of DFRCC specimen is lower than that of mortar specimen. This reason will be discussed. The cracks in DFRCC specimen are narrower width and shallower depth than those in mortar specimen, as described in 2.2. Therefore, oxygen and water which are needed for the cathodic corrosion reaction are fewer in DFRCC specimen, compared to mortar specimen. Therefore, the corrosion rate of DFRCC specimen is lower than that of mortar specimen. Additionally, the local corrosion rate is generally high in case of macrocell. While, the corrosion rate is low which in case of microcell. Therefore, based on the above result of the corrosion cell formation pattern, the corrosion rate of DFRCC specimen is lower than that of mortar specimen.

5 CONCLUSIONS

In this study, the chloride induced corrosion or the carbonation induced corrosion is compared between normal mortar and DFRCC using specimen with bending cracks under the accelerated environment. The conclusions are as follows.

1) The corrosion cell formation pattern of mortar is macrocell. On the other hand, that of DFRCC is the microcell.
2) The corrosion rate of DFRCC is lower than that of mortar.
3) The penetration of chloride ions or CO_2 in the crack of DFRCC is shallower than that of mortar.
4) The durability for chloride induced corrosion or carbonation induced corrosion is higher in DFRCC, compared to mortar.

ACKNOWLEDGMENT

The authors are grateful to T. Kamada, Dr. Eng and M. Kunieda, Dr. Eng for their advice, and also to Mr. T. Honma and Mr. M. Hakoyama for their cooperation.

REFERENCES

[1] V. C. Li, and T. Kanda, “Engineered Cementitious Composites for Structural Applications” ASCE J. Materials in Civil Engineering, Vol.10, No.2, pp.66-69, 1998.

[2] M. Kunieda, T. Kamada, and K. Rokugo, “Size Effects on Flexural Failure Behavior of ECC Members” the proceeding of the JCI International Workshop on Ductile Fiber Reinforced Cementitious Composites, 2002.

[3] N. Otsuki, S. Miyazato, Nathaniel B. Diora, and H. Suzuki, “Influences of Bending Crack and Water-Cement Ratio on Chloride-induced Corrosion of Main Reinforcing Bars and Stirrups” ACI MATERIALS JOURNAL, Vol.97, No.4, pp.454-464, 2000.

[4] T. Tsuru, R. Maeda, and S. Haruyama, “Application of A-C corrosion monitor to localized corrosion” Corrosion Engineering, No.28, pp.638-644, 1979. (in japanese)